

F.E. Cecil, V. Kiptily, A. Salmi, A. Horton, K. Fullard, A. Murari,
D. Darrow and K. Hill

Analysis of and Proposed Solution for the Anomalous Currents in the Front Foils of the JET Lost Alpha Particle Diagnostic KA-2

"© – COPYRIGHT ECSC/EEC/EURATOM, LUXEMBOURG – 2008"

"Enquiries about Copyright and reproduction should be addressed to the
Publications Officer, EFDA, Culham Science Centre, Abingdon, Oxon, OX14 3DB, UK."

Analysis of and Proposed Solution for the Anomalous Currents in the Front Foils of the JET Lost Alpha Particle Diagnostic KA-2

F.E. Cecil¹, V. Kiptily², A. Salmi², A. Horton², K. Fullard², A. Murari²,
D. Darrow³ and K. Hill³

¹*Colorado School of Mines, Golden, Colorado USA*

²*EURATOM/UKAEA Fusion Association, Culham Science Centre, OX14 3DB, UK.*

³*Princeton Plasma Physics Laboratory, Princeton, New Jersey, USA*

Analysis of and proposed solution for the anomolous currents in the front foils of the JET lost alpha particle diagnostic KA-2

F.E. Cecil¹, V. Kiptily², A. Salmi², A. Horton², K. Fullard², A. Murari², D. Darrow³ and K. Hill³,

1. Colorado School of Mines, Golden, Colorado USA

2. Euratom/UKAEA Fusion Assoc., Culham Science Center, Abingdon Oxon, UK

3. Princeton Plasma Physics Laboratory, Princeton, New Jersey, USA

Abstract

We have examined the observed currents in the front foils of the JET Faraday cup lost alpha particle diagnostic KA-2. In particular we have sought to understand the currents during Ohmic plasmas for which the ion flux at the detectors was initially assumed to be negligible. We have considered two sources of this current: plasma ions (both deuterium and impurity) in the vicinity of the detector (including charge exchange neutrals) and photoemission from scattered UV radiation. Based upon modeling and empirical observation, the latter source appears most likely and, moreover, seems to be applicable to the currents in the front foil during ELMy H-mode plasmas. A very thin gold or nickel foil attached to the present detector aperture is proposed as a solution to this problem and realistic calculations of expected fluxes of lost energetic neutral beam ions during TF ripple experiments are presented as justification of this proposed solution.

1. Introduction

The JET EP-1 diagnostic KA-2 consists of sets of thin (2.5 μm) Ni foils mounted in a poloidal array near the plasma boundary in octant 7 of the JET tokamak. A photograph of the JET interior showing KA-2 is shown in Figure 1. The design and operating principles of KA-2 are given elsewhere [1]. KA-2 was recently commissioned as a diagnostic for lost alpha particles during d-t plasmas [2]. Pending such plasmas we have sought to utilize KA-2 as a diagnostic of lost energetic particles from deuterium plasmas during, for example, neutral beam (NBI) and ion cyclotron radio frequency (ICRH) heated plasmas. Deuterons with energies up to 500 keV will stop in the front foil of the KA-2 detectors and hence the analysis of lost NBI ions is necessarily limited to an examination of the currents in these front foils. During the course of our examination of the front foil currents, we have repeatedly observed currents during the Ohmic phases of the tokamak plasma where ion temperatures are limited to a few keV. An example of such a plasma is given in Figure 2. In this report we discuss possible sources of this anomalous current and propose a solution. In addition we report realistic calculations of NBI losses which suggest that the proposed solution would allow the observation of these losses. Since devices comparable to KA-2 have been installed on DIII-D [3] and NSTX [4] and are being considered as a lost alpha particle diagnostic for ITER [5], it may be useful to consider the present proposed solution in the context of these machines.

2. Possible sources of anomalous current

Three sources of current during Ohmic plasmas are considered:

- 1) Thermal plasma in the immediate vicinity of the detector
- 2) Neutral ions becoming re-ionized near the detector
- 3) Photo-emission from the front foils due to scattered UV radiation

a) Thermal plasma in the immediate vicinity of the detector

This plasma may be assumed to consist of deuterium ions as well as impurity ions (e.g. Carbon, Oxygen, and Beryllium). The detector is located about 3 cm from the plasma edge and hence the densities and temperatures should be fairly low. The minimum energy at which a given ion can reach the front foil may be roughly estimated assuming by a pitch angle of 45° (geometrically the minimum pitch angle for which the ion can both enter a top hole of the aperture and still strike the foil. In addition the ion must travel a distance of 8 mm (the distance from the edge of the detector to the nearest aperture within one half of a complete gyro-orbit. The geometry of this relationship is sketched in Figure 3. In this figure the particle is launched at the top edge of the detector with its velocity on the y-z plane at a pitch angle $\theta_{\text{pitch}} = 45^\circ$. After one half of gyro-orbit it arrives at the near edge of one of the aperture holes with diameter 3 mm and with a pitch angle of 45° below the plane of the detector. It will strike the foil at a depth 3 mm below the top surface of the detector. The distance it has traversed is πr_{gyro} . The corresponding minimum energy (in keV) is given by:

$$T_{\text{min}} = 0.311 B^2 / m$$

where B is in Tesla and m is in amu (2.014 for a deuteron, 12 for Carbon) . Since the trajectory for the particle indicated in Figure 3 as it enters the hole will be starting to curve upward, the estimate given above is low by about 40%.

A more realistic estimate of the energies required for a given ion to reach the front foil of the detector and the associated currents that one could expect for a given ion density are determined using a MONTE-CARLO code in which a ion is launched randomly within a 1 cm by 1 cm x 1 cm rectangular prism at some height H above the front surface of the aperture. The geometry of this model is sketched in Figure 4. The coordinate system is the same as in Figure 3. The ion is launched with spatially isotropic pitch and cyclotron angle. A constant $B = 1.7$ T is assumed along the z -axis. In the calculation we assume a complete array of 8 (x-direction) x 17 (z-direction) 3 mm diameter holes with a center to center separation of 4 mm. We find that at 50 keV the probability of a deuteron reaching the front foil is about 0.6 %. The probabilities as a function of energy for deuterons and Carbon with the height $H = 1$ cm are plotted in Figure 5. At the lowest energies, the probability of detecting a carbon ion exceeds that of a deuteron by virtue of the larger gyroradius. In addition the region of space from which a carbon ion might strike a front foil exceeds that of a deuterium ion of the same energy, again by virtue of the greater gyroradius. The results of modeling this difference is shown in Figure 6.

These probabilities from Figure 5 may be used to calculate the currents measured in the front foil by recognizing that all the ions in a column of dimension (1 cm x 1 cm x $V_{z_{av}}$) will enter the 1 cm³ region next to the detector in

1 sec. For a 50 keV deuteron, $V_{z_{av}} = 1.26 \cdot 10^8$ cm/sec while for a 50 keV carbon ion, the average speed is $5.15 \cdot 10^7$ cm/sec. The above probabilities scaled by the gyroradius to account for the volume effect shown in Figure 6 will determine the number of ions entering the front foil (per aperture hole) at unit plasma density assuming a monoenergetic plasma. These currents, per aperture hole, are plotted in Figure 7. Also shown in Figure 7 are empirical fits to the modeled current values.

For a thermal rather than monoenergetic plasma, the currents may be integrated over a normalized Maxwell-Boltzmann distribution to obtain the current as a function of temperature. At the location of the detectors, the plasma density is about 10^{12} cm⁻³ [6] for the shot given in Figure 2 at a time of 55 sec and Z_{eff} is about 1.5. Hence we assume a deuterium density of $9 \cdot 10^{11}$ cm⁻³ and a carbon density of 10^{11} cm⁻³. The predicted currents associated with the deuterium and carbon components of this plasma as a function of temperature are given in Figure 8. In Figure 9, the temperature for shot 69608 is plotted for the location of the detector KA2-411. During the Ohmic phase of the shot we find a temperature of 25 eV and hence from Figure 8 would expect a current of about 1 nA, due almost entirely from the carbon. During the NBI for this shot the temperature rises to about 40 eV and the expected current to about 20 nA. In all cases the expected currents are well below the measured current of between 3 and 5 μ A and are dominated by the impurity ions. Further evidence against the front foil signals arising from plasma impurities is suggested in Figure 10 by the lack of correlation between the current in the front foil KA2-411 and the horizontal and vertical CIII

cameras DD/S3-AD13 and DD/S3-AD15. Hence we conclude that for low temperature plasmas such as 69608, the possibility of the observed currents in the KA2 front foils arising from plasma ions must be discounted. It should be noted, however, again referring to Figure 8, that at temperatures in excess of 0.1 keV, the expected currents of plasma impurity ions at the front foils for impurity densities of 10^{11} cm^{-3} will exceed $1 \mu\text{A}$

2) Neutral ions becoming re-ionized near the detector

Alternatively we might consider charge exchange neutral ions in the detector vicinity. This was proposed by Jarvis et al. [7] to explain the observed currents in the front foil of KA-1 during ICRH and neutral beam heated plasmas on JET from 1995 until 2000. The neutral ion flux during the Ohmic phase of 69707 is about $10^{10} \text{ cm}^{-2} - \text{sec}^{-1}$ [8] and as such would not be capable of generating microAmperes of current in the KA-2 front foils even if all the neutrals were reionized. This possible source of the KA2 front foil currents during Ohmic plasmas is likewise discounted.

3) Photo-emission from the front foils due to scattered UV radiation

Finally we consider the possibility of the photoemission from the front foil by reflected UV radiation. (The apertures were designed to face away from any direct line of sight to exclude hard x-rays from entering the detectors; however there is a direct line of sight from the foils in the second through fifth poloidal locations to the bottom of the next higher pylon). The plausibility of this

mechanism is suggested by comparing the measured front foil current to the plasma bolometric radiation which is a good measure of the total UV radiation from the plasma. The current in KA2-411 and the signal from the bolometer diagnostic BOLO/TOPI is shown in Figure 11 where the relative concordance of the two signals is to be noted. As seen in this Figure 12, there is an approximately linear relation between the current in KA2-411 and the total radiated power as measured by BOLO/TOPI for a number of JET pulses over nearly three orders of magnitude with a proportionally constant between I_{411} and bolometric radiation of about $8 \mu\text{A}/\text{MW}$. It should be stressed that the data in Figure 12 includes ELMy H-mode plasmas at the highest bolometry powers (100 MW). Since the same proportionality with the KA2 front foil current obtains at these high powers, it would appear that the front foil currents are associated with scattered UV radiation over this very broad dynamic range. The source of the current in this model is then that photoelectrons are ejected from the surface by the UV photons and this loss of negative charge from the foil is measured as a positive current. This hypothesis may be tested by inserting a small battery in the circuit between the foil and the current amplifier which feeds the diagnostic digitizer. This would provide a positive bias to the foil which would prevent the photoelectrons from leaving the foil. In addition other electrons from the environment would be attracted to the foil causing a negative current to be measured. This is indeed what was observed as seen in Figure 13. In addition, this model is especially supported by the fact that the KA2 front foil current-to-bolometric power ratio with a negative voltage of 1.5 V is about the same as with no voltage.

We may estimate the expected current from UV photoemission by considering the UV scattered into the front foil of KA2-411 from the back of the pylon for KA2-311 which is located approximately 10 cm from the KA2-411 front foil and is tilted at an angle of 45° to the minor radius of the tokamak. Assuming an average energy of the UV radiation of 10 eV, a reflectance of the inconel pylon of 20% [9], we estimate a reflected UV power onto the front aperture of KA2-411 of $0.025 \text{ W}/(\text{cm}^2 \text{--MW})$. From this power, assuming a quantum efficiency of 10^{-4} [10], would estimate a current in KA2-411 of about $2 \mu\text{A}/\text{MW}$ of bolometric power; this is within an order of magnitude of the observed relation of $8 \mu\text{A}/\text{MW}$.

On the basis of this order of magnitude agreement and given the response of the system to the low voltage batteries, and given the qualitative and quantitative disagreement between the measured currents and predicted signals from plasma ions and reionized neutrals, we feel confident that the source of the anomalous currents in the front foils of KA-2 during Ohmic plasmas is primarily the result of photoemission from scattered UV radiation.

3. Proposed solution

Probably the simplest solution to the problem of the anomalous currents in the front foils of KA-2 is to install a very thin foil in front of the aperture which would eliminate the scattered UV (as well as any plasma ions which, as noted above may contribute to the front foils currents during high temperature plasmas) while allowing relatively energetic ions, such as beam ions with energies ~ 100 keV, to reach the front foils. Considering a foil of thickness $0.1 \mu\text{m}$, deuterons with energy less than 14 keV will stop in Ni while deuterons of energy less than 27 keV will stop in Au. The shielding against impurity atoms is even more effective with C ions of energy up to 90 keV stopping in $0.1 \mu\text{m}$ of either foil. On the other hand 100 keV deuterons from NBI will lose less than 20 keV in either $0.1 \mu\text{m}$ foil. Similarly the energy loss of the 3.5 MeV alpha particles from d-t plasmas will only lose about 50 keV in either $0.1 \mu\text{m}$ foil. [11]. In terms of the protection of the front foils of KA-2 from the scattered UV radiation discussed above, the transmission of 10 eV UV radiation will be roughly 10^{-9} [9]. Thus a gold or nickel foil of thickness $0.1 \mu\text{m}$ can be placed in front of KA-2 and will eliminate low energy deuterons, impurity ions and UV radiation without compromising the study of fast ions such as NBI deuterons and d-t lost alphas.

Although the proposed $0.1 \mu\text{m}$ foil will eliminate thermal plasma ions and scattered UV radiation from the front foils of KA-2, it is essential to consider whether the heat load associated with this radiation poses a threat of melting of the foil (given the melting temperatures of 1337 K for gold and 1726 K for nickel). We have investigated this possibility by constructing a 2-dimensional

finite element heat transfer model to take account of heating by incident radiation and cooling by black body radiation and thermal conductivity to the foil support structure which is assumed to remain at an ambient temperature of 600 K. The temperature of either a gold or nickel foil exposed to a 20 ms pulse of 0.025 W/mm^2 (the expected flux if the total bolometric radiative power is 100 MW) is shown in Figure 14. While such a large radiative power would be extraordinarily high in steady state, it is encountered briefly (few ms) during the ELMS in H-mode plasmas. The temperature in Figure 14 is calculated for a 20 ms pulse to give an assurance that the asymptotic temperature of the foils under even extreme conditions is well below the melting temperatures. Nonetheless, prudence would dictate the use of Ni foils rather than Au by virtue of the greater melting temperature.

While the proposed solution appears to provide a heat resistant mechanism for the elimination of the anomalous currents in the KA-2 front foils, it is important to address the issue of whether we would expect to make useful measurements prior to any d-t operation in the absence of these currents. We believe such measurements can be made. Using the fully collisional orbit code ASCOT we have calculated the currents into the front foils of KA-2 during high and low triangularity H-mode plasmas with 1% toroidal field ripple. We compare these calculations with measured currents (the quiescent currents between the ELMS) in KA-2. This comparison is shown in Figure 15. where it is noted that the peak predicted losses are well in excess of a nanoAmp and should be readily

measured if the anomalous currents are eliminated with the proposed thin foil. We would emphasize that the two low calculated values ($\sim 10^{-4}$ uA) represent upper limits. In addition we would emphasize that the estimates in Sec. 2 of this report applied to KA2-411 and that the fluxes of scattered UV radiation at the other front foils will vary from that of KA2-411 by virtue of detector environment, inclination of the detector, spatial distribution of the source of the primary UV radiation, etc. A consideration of these factors in an effort to understand the present poloidal distribution of the front foil currents is in progress and will be reported on at a later date.

4. Conclusion

We propose the installation of very thin (0.1 μm) Ni foils in front of the existing apertures to the JET lost alpha particle diagnostic KA-2. These foils would eliminate scattered UV radiation as well as deuteron and impurity plasma currents from the KA-2 front foils and allow the study, for example, of lost neutral beam ions during TF ripple experiments on JET. The foil temperatures would not approach melting even at extreme UV fluxes. Finally we would like to emphasize that the present background signal in the front foils does not compromise the reliability of KA-2 as a diagnostic of lost alpha particles from d-t plasmas since these alpha particles will generally stop in the second and third foils. As illustrated in Figure 16, the second foil KA2-132, for example, maintains a quiescent background of $I_{\text{rms}} < 1 \text{ nA}$ while the front foil KA2-131 is recording microAmperes.

We wish to acknowledge a number of very helpful conversations with Guy Matthews, Gunaddy Sergienko and Kerry Lawson in the consideration of this problem. In addition this work is supported in part by a grant from the US DOE.

References

1. D. S. Darrow, F. E. Cecil, V. Kiptily, R. Ellis, L. Pedrick , S. Baumel and A. Werner, Rev. Sci. Instrum. **75** , 3566 (2004).
2. <http://users.jet.efda.org/pages/codes-data/dvcm/meetings/27-Mar-2008/index.htm>
3. W.P. West, C. Lasnier, J.G. Watkins, J.S. deGrassie, W.W. Heidbrink, K.H. Burrell and F.E. Cecil. J. Nucl. Materials, **420** , 337 (2005). F.E. Cecil, A. Aakhus-Witt, J. Hawbaker, J. Sayers, A. Bozek, W. Heidbrink, D. Darrow, T. Debay, E. Marmar, “Thin foil Faraday collectors as a radiation hard lost fast ion diagnostic”. Reviews of Scientific Instruments. **74**. 1747
4. D.S. Darrow, , R. Bell, D.W. Johnson, H. Kugel, J.R. Wilson, F.E. Cecil,R. Maingi, A. Krasilnikov and A. Alekseyev. Rev. Sci. Instrum.,**72**, 784 (2001). W. Heidbrink, M Miah, D Darrow, B LeBlanc, S S Medley, A L Roquemore and F E Cecil . Nuclear Fusion **43**, 883 (2003).
5. M. Sasao et al. Plasma Phys. Control. Fusion **46** , S107 (2004).
6. The edge plasma density is calculated by the JET utility RADISPLAY.
7. O.N. Jarvis, P. v. Belle, M. Hone, G. Sadler, G. Whitfield, F.E. Cecil, D.S. Darrow and B. Esposito, Fusion Technology **39**, 84 (2001).
8. V. Afanasyev, private communication (2008)
9. H.J. Hagemann, W. Gudat and C. Kunz. Deutsches Elektronen-synchrotron Report DESY – SR-7417 (1974)

10. R.L. Farquart, B. Ray and J.D. Swift. J. Phys. D: Appl. Phys **13** , 2067 (1980)

11. These range and stopping power calculations were carried out with

SRIM2006.

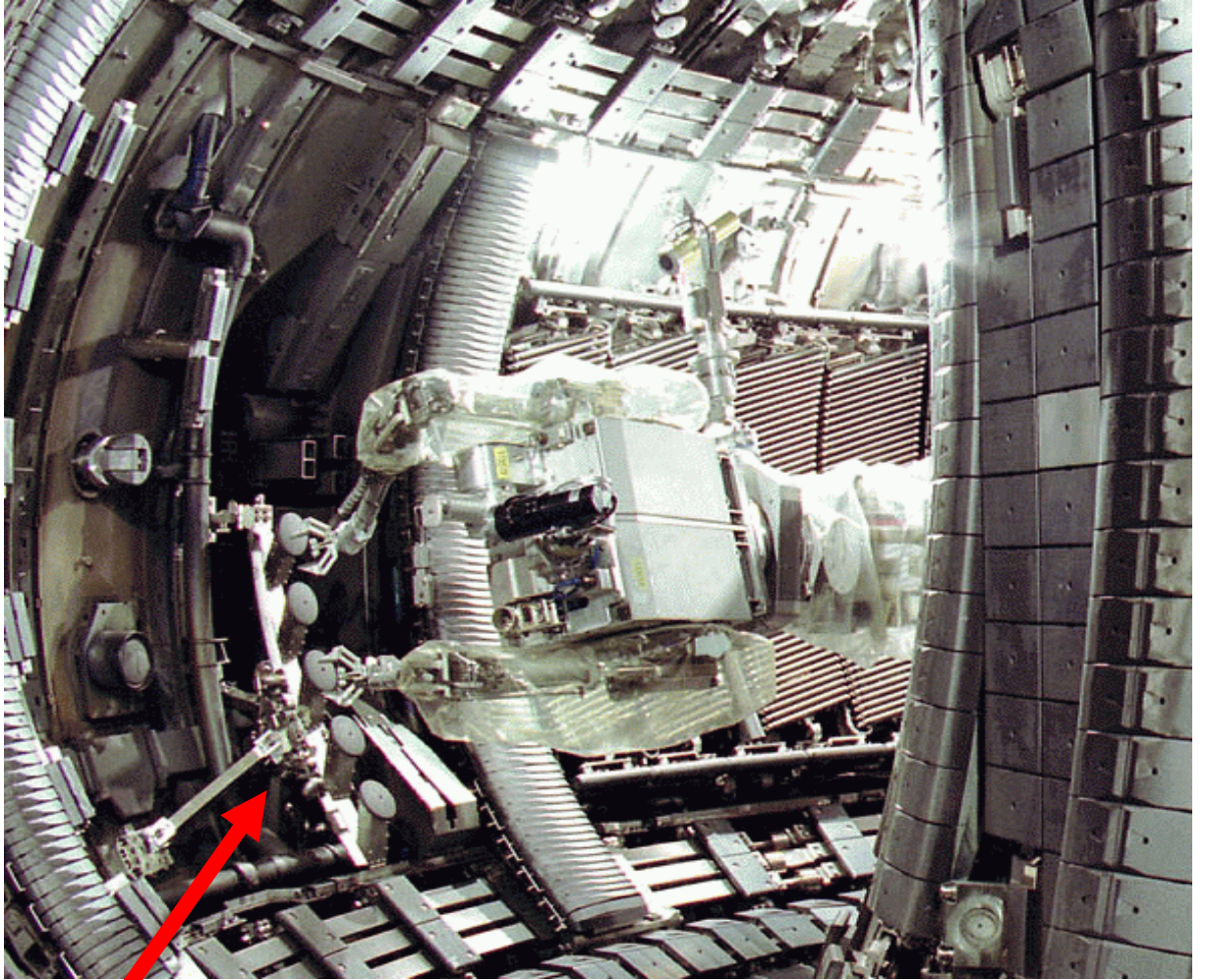


Figure 1 Photograph of JET interior showing lost alpha particle diagnostic with its five poloidal locations being installed May 2005.

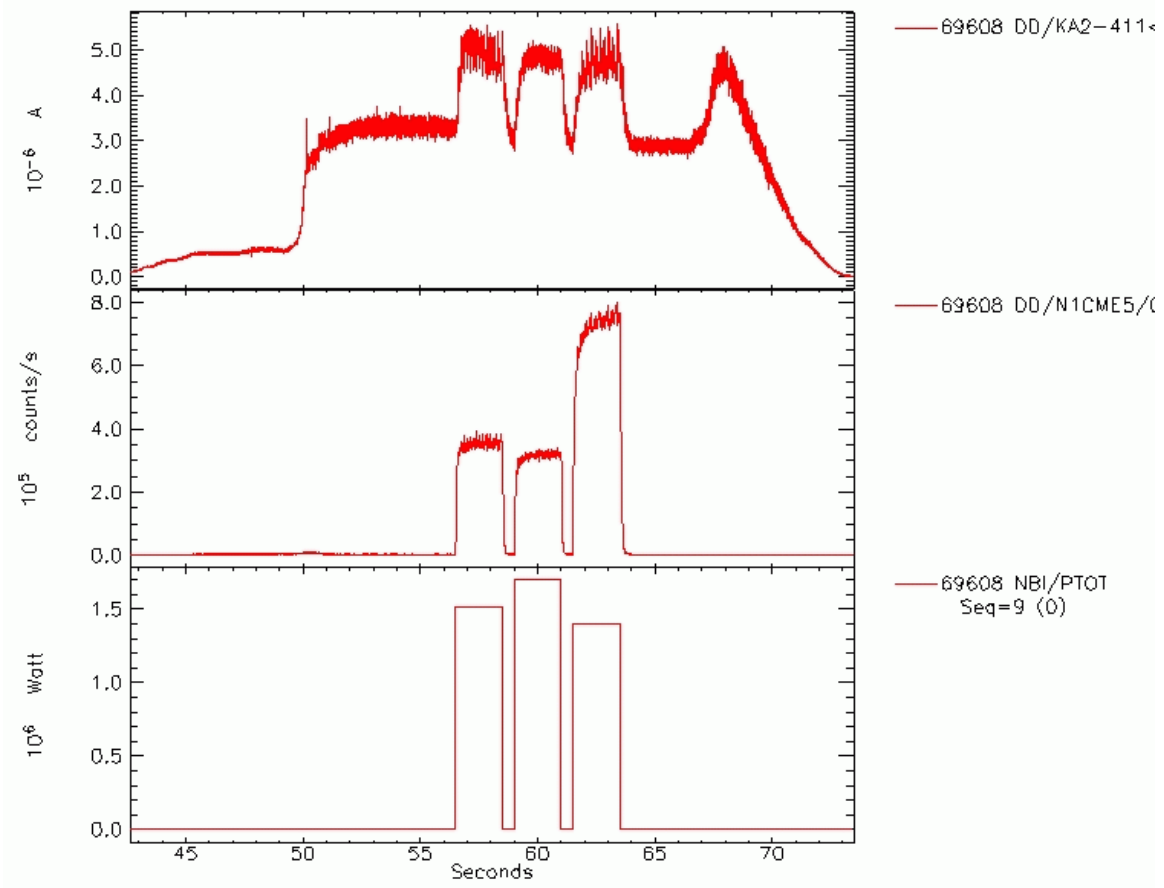


Figure 2. Comparison of the current in KA2-411 with neutron yield and NBI power. The μ A currents during the Ohmic phase of the shot ($t < 56$ sec) are to be noted

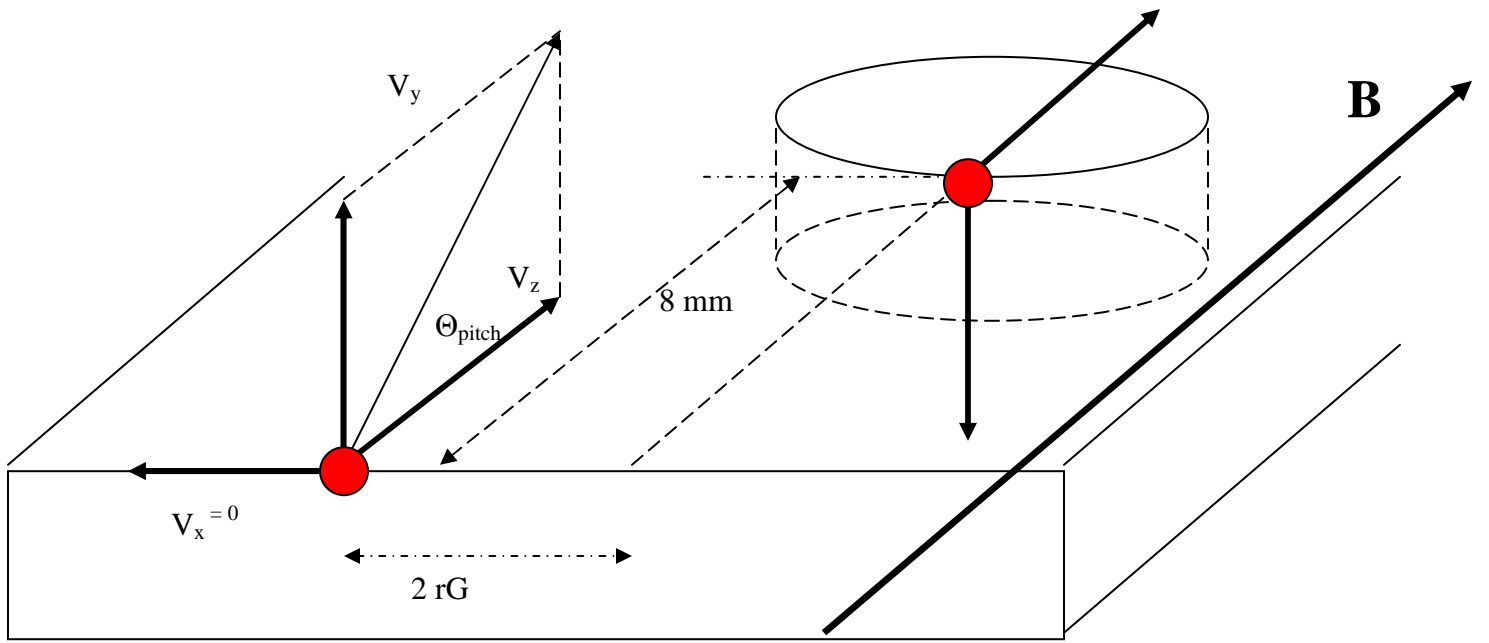


Figure 3. Schematic diagram of aperture to detector with one hole indicating initial and final location of an ion starting at the edge of the detector and arriving at one corner of the hole.

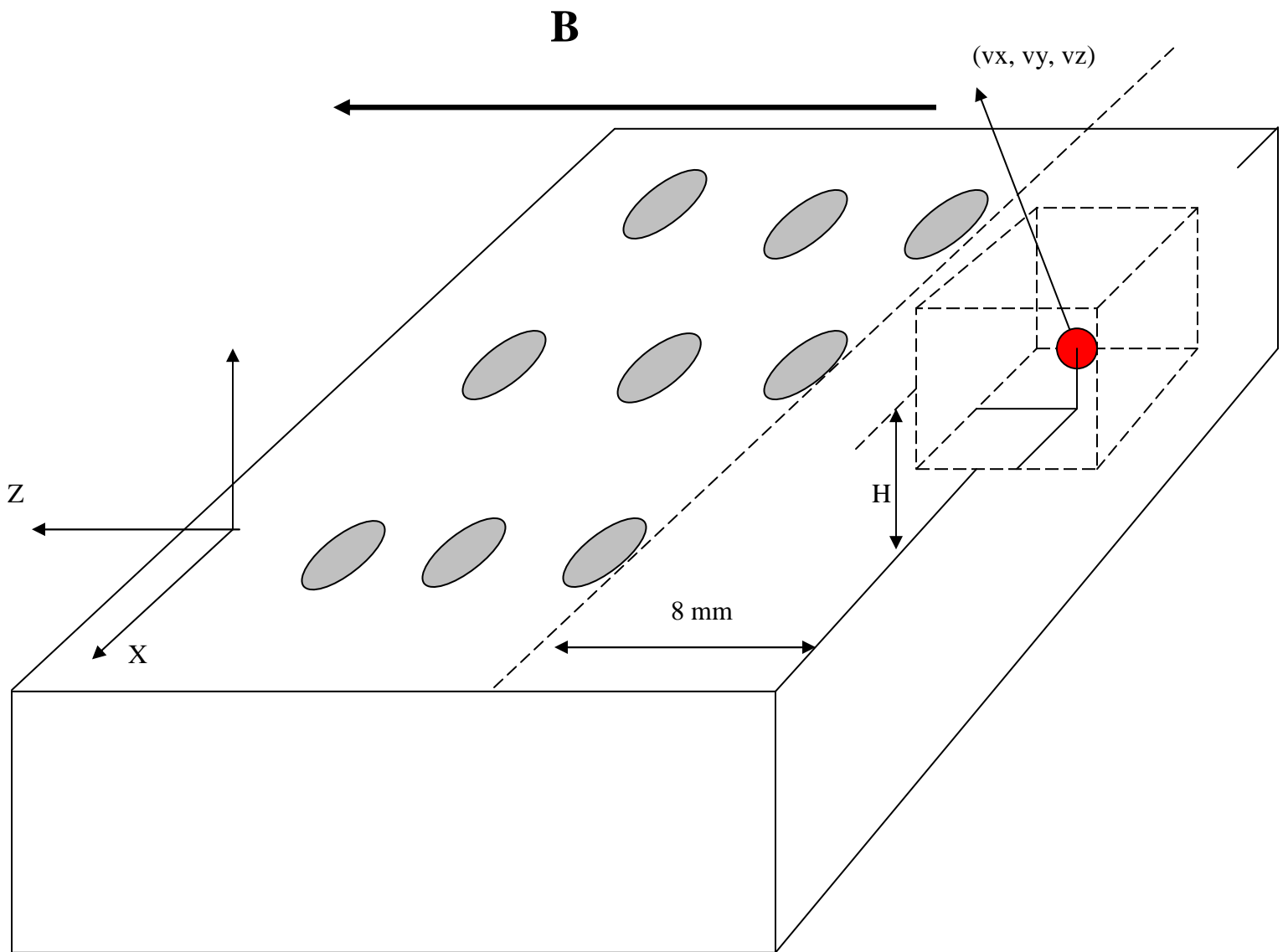


Figure 4 Schematic diagram of detector illustrating the geometry of the MONTE-CARLO code used to calculate the probability of an ion in the vicinity of the detector reaching the front foil,

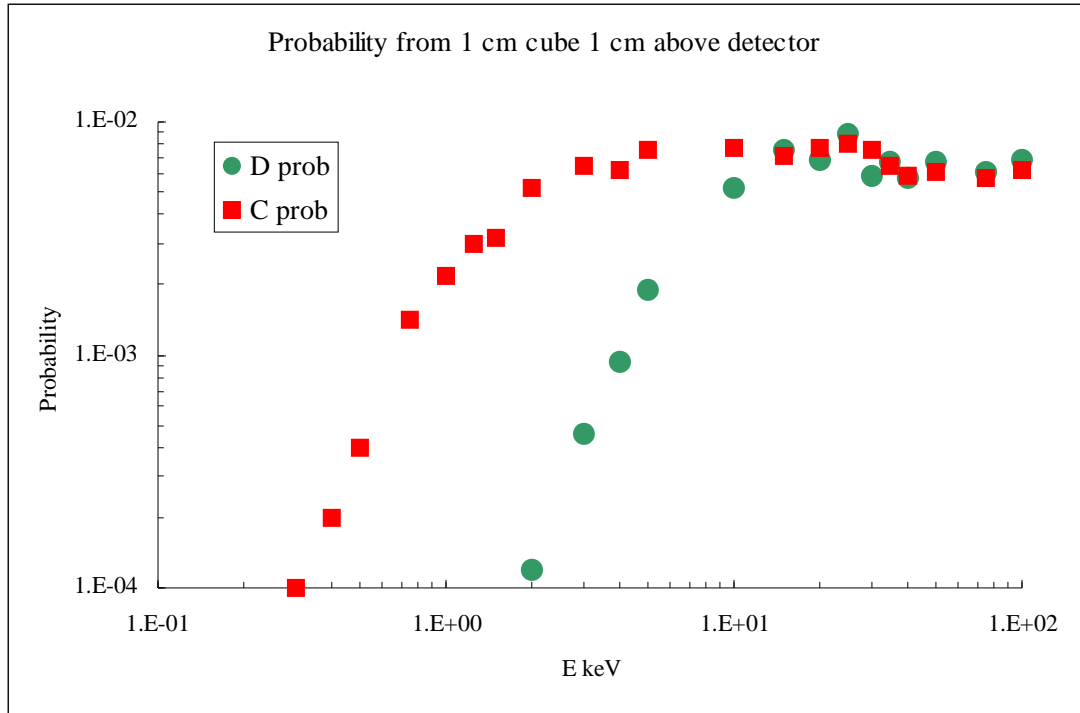


Figure 5. Calculated probabilities for carbon and deuterium ions randomly launched from a 1 cm cube whose center is 1 cm above the front surface of the aperture. The carbon has a much greater probability than the deuterium at low energies by virtue of the greater gyroradius.

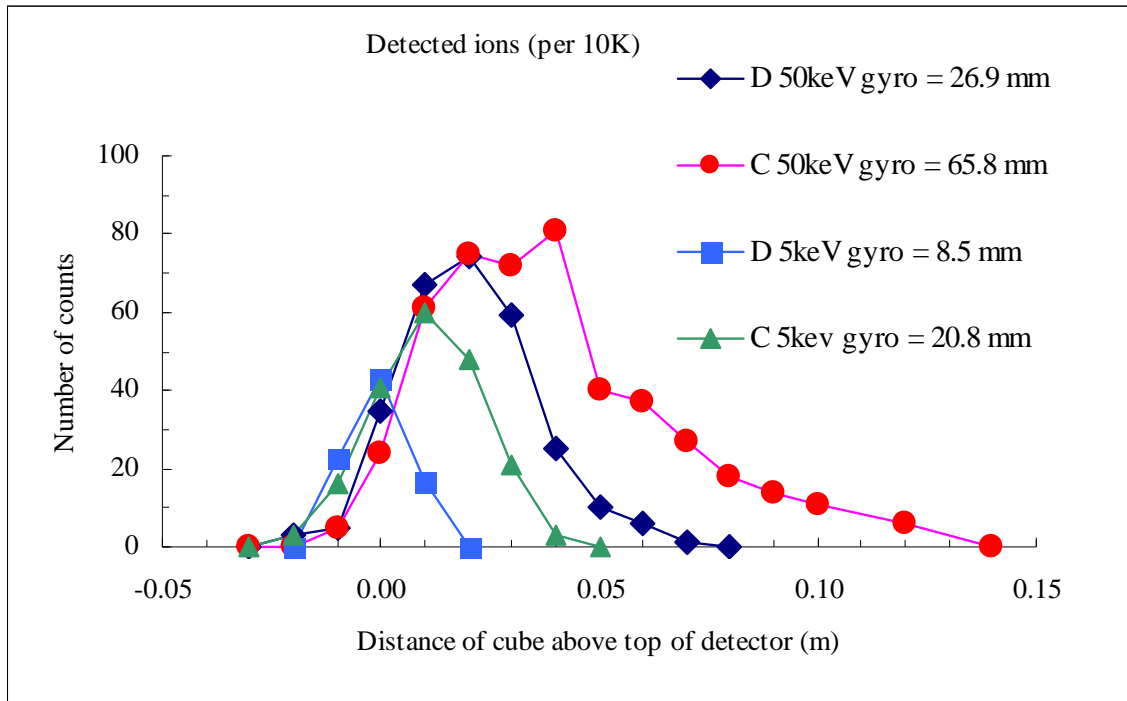


Figure 6. Number of ions reaching the front foils from a 1 cm cube as a function of the height of the center of the cube above the front surface of the aperture.

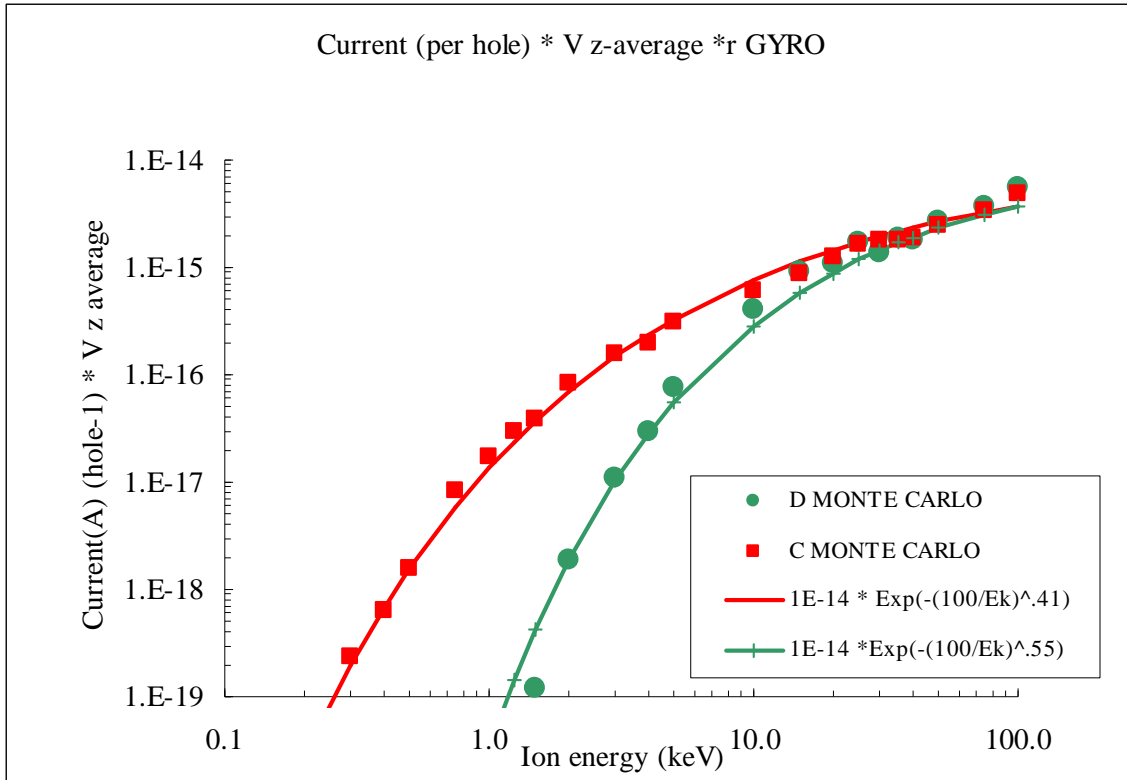


Figure 7. The ion current for a monoenergetic deuterium or carbon plasma of unit density.

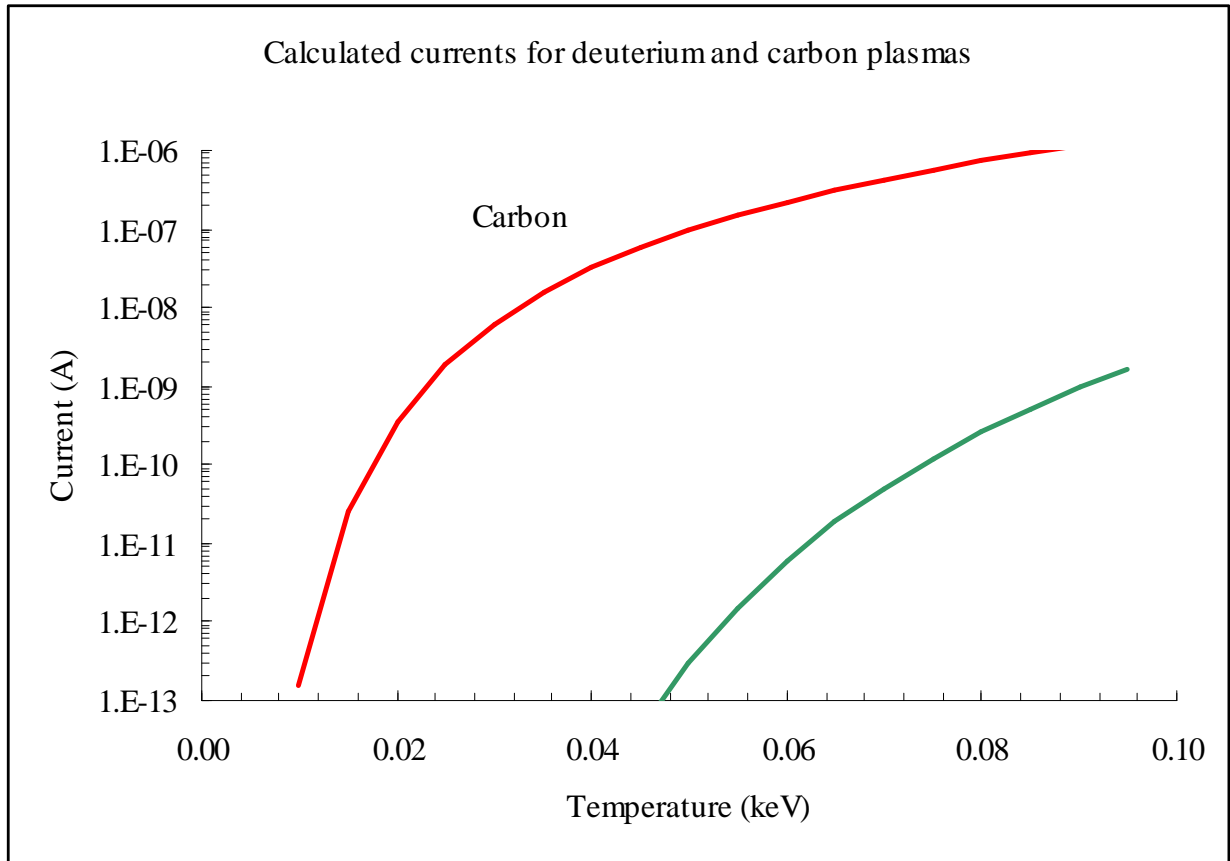


Figure 8. The ion currents from the deuterium and carbon ions for thermal plasmas of total density 10^{12} cm^{-3} and a $Z_{\text{eff}} = 1.5$.

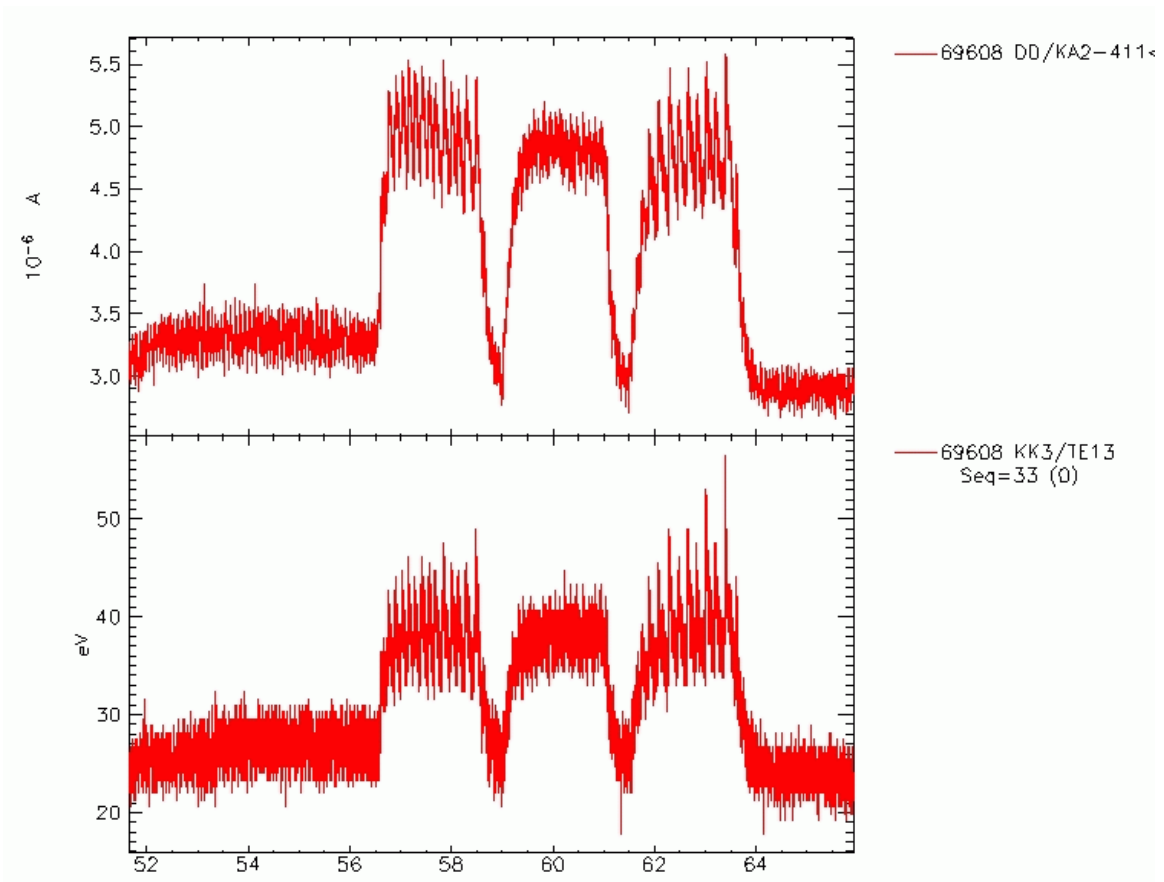


Figure 9 The electron temperature at the location of KA2-411 for shot 69608.

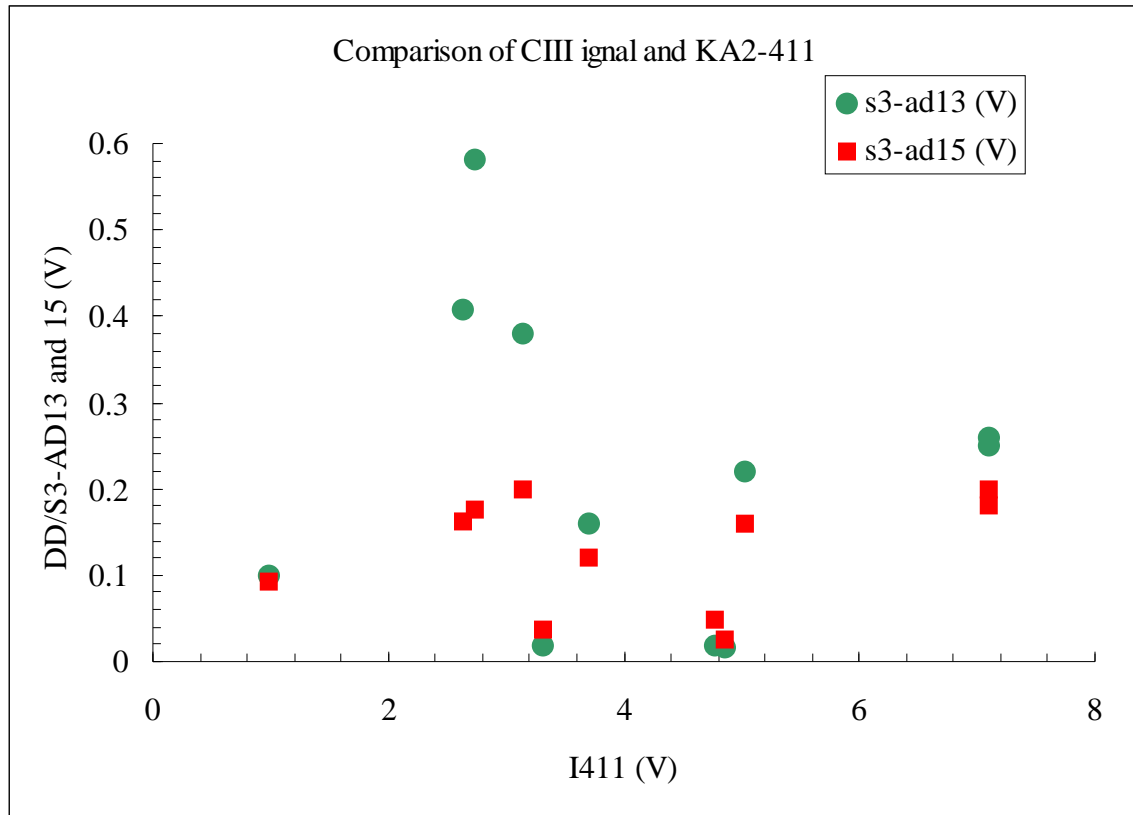


Figure 10. A comparison of the horizontal and vertical CIII signals and the current in KA2-411.

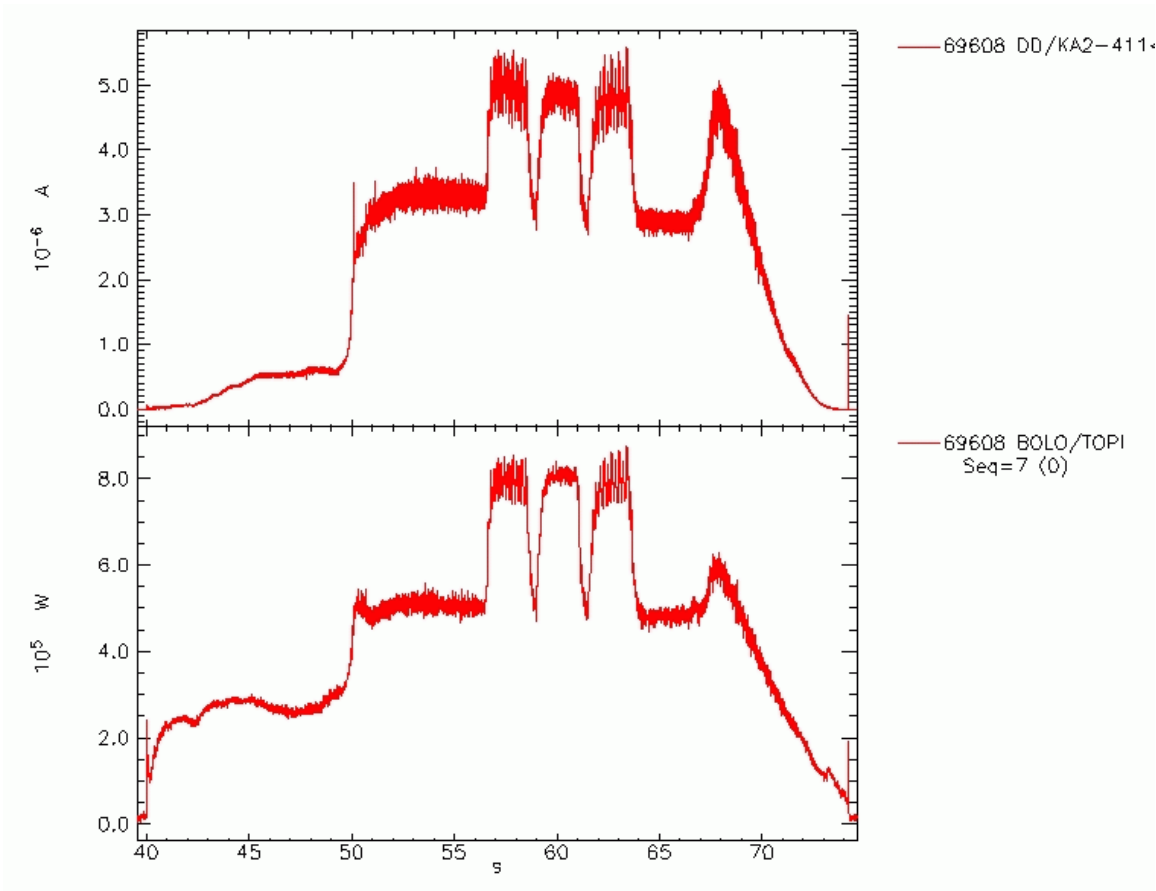


Figure 11 A comparison of the current in KA2-411 and the total radiated bolometric power BOLO/TPOI.

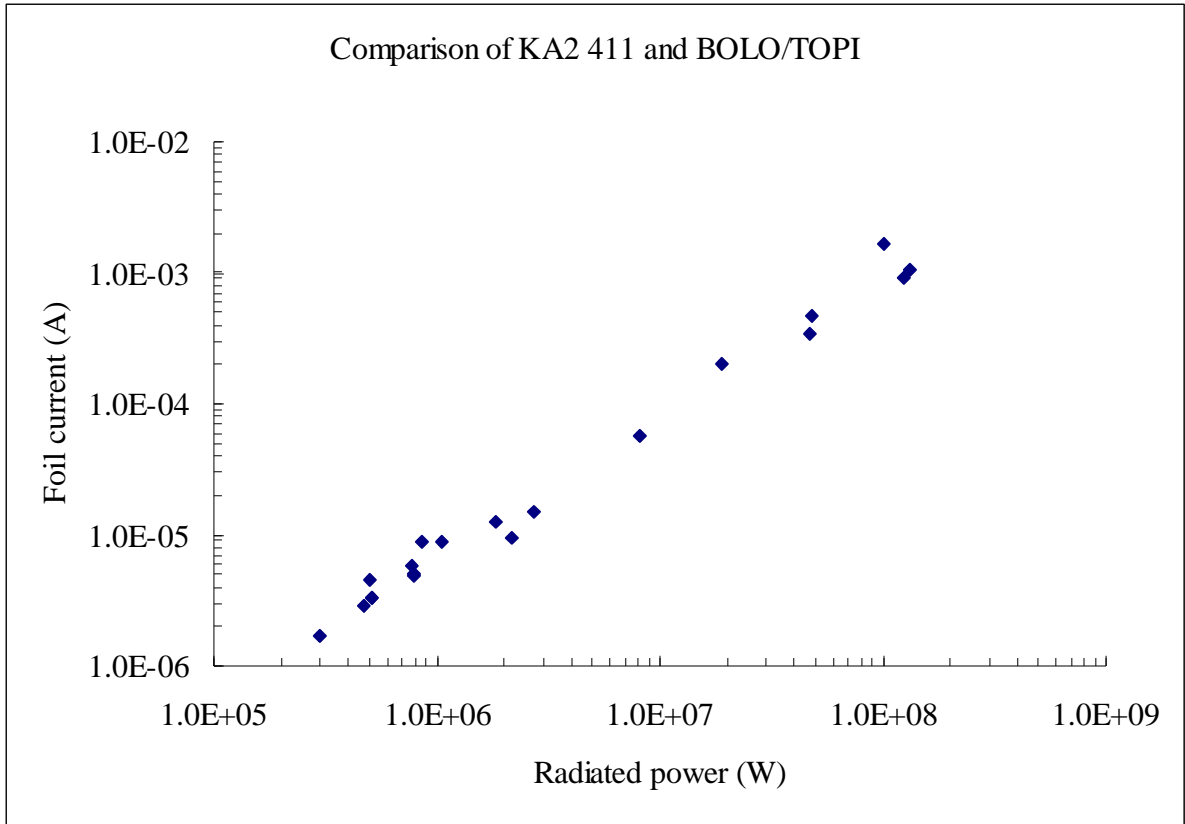


Figure 12. A comparison of the current in KA2-411 and the total bolometric power BOLO/TOPI for plasmas from Ohmic to ELMy H-mode.

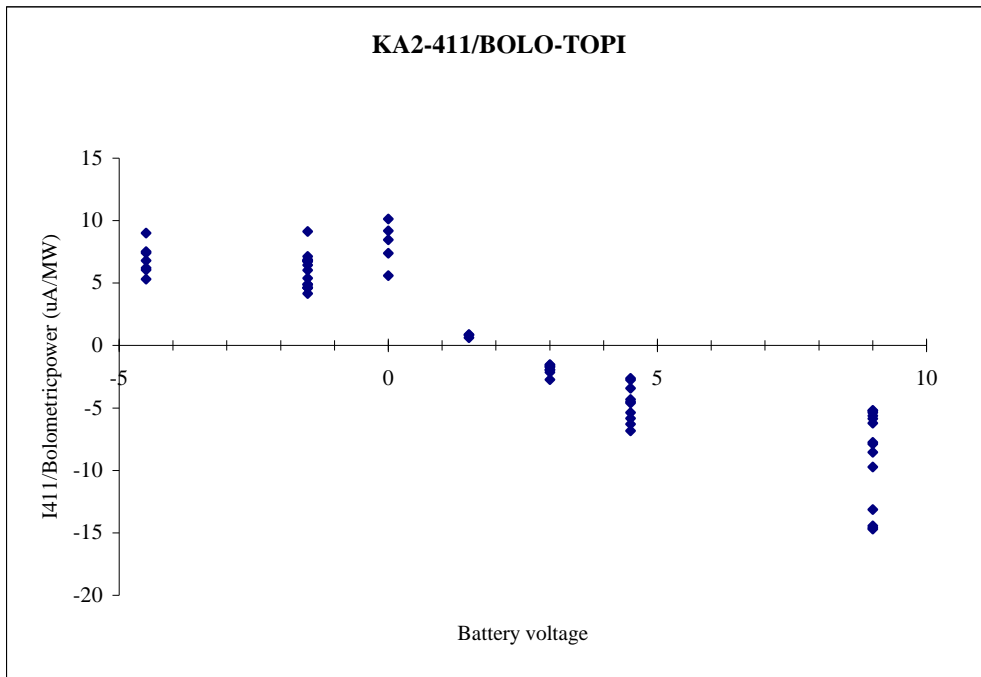


Figure 13. The ratio of KA2-411 current to the total bolometric power as a function of the voltage of a battery placed in the line from the foil to the amplifier to suppress electrons from being ejected from the foil surface by scattered UV radiation.

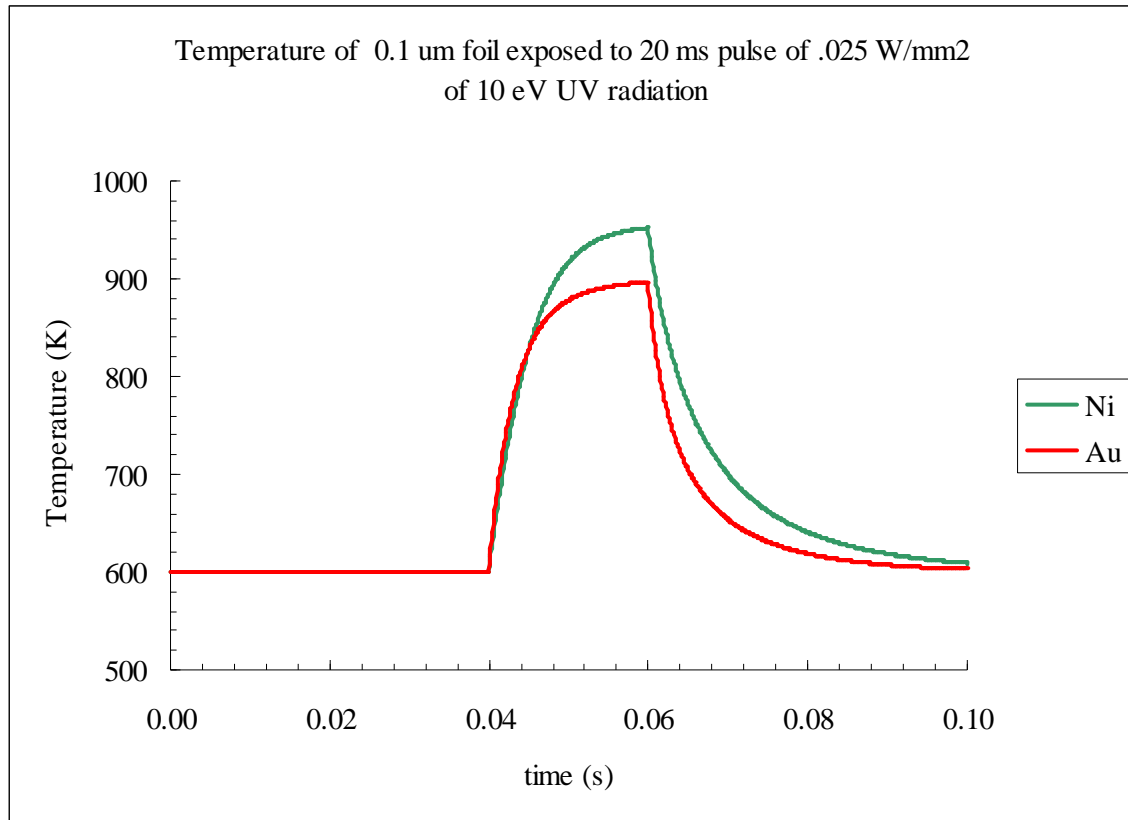


Figure 14. The temperatures of Au and Ni foils exposed to a 20 ms pulse of 0.025 W/mm^2 of UV radiation. This assumes the edge of the foils is maintained at an ambient temperature of 600 K.

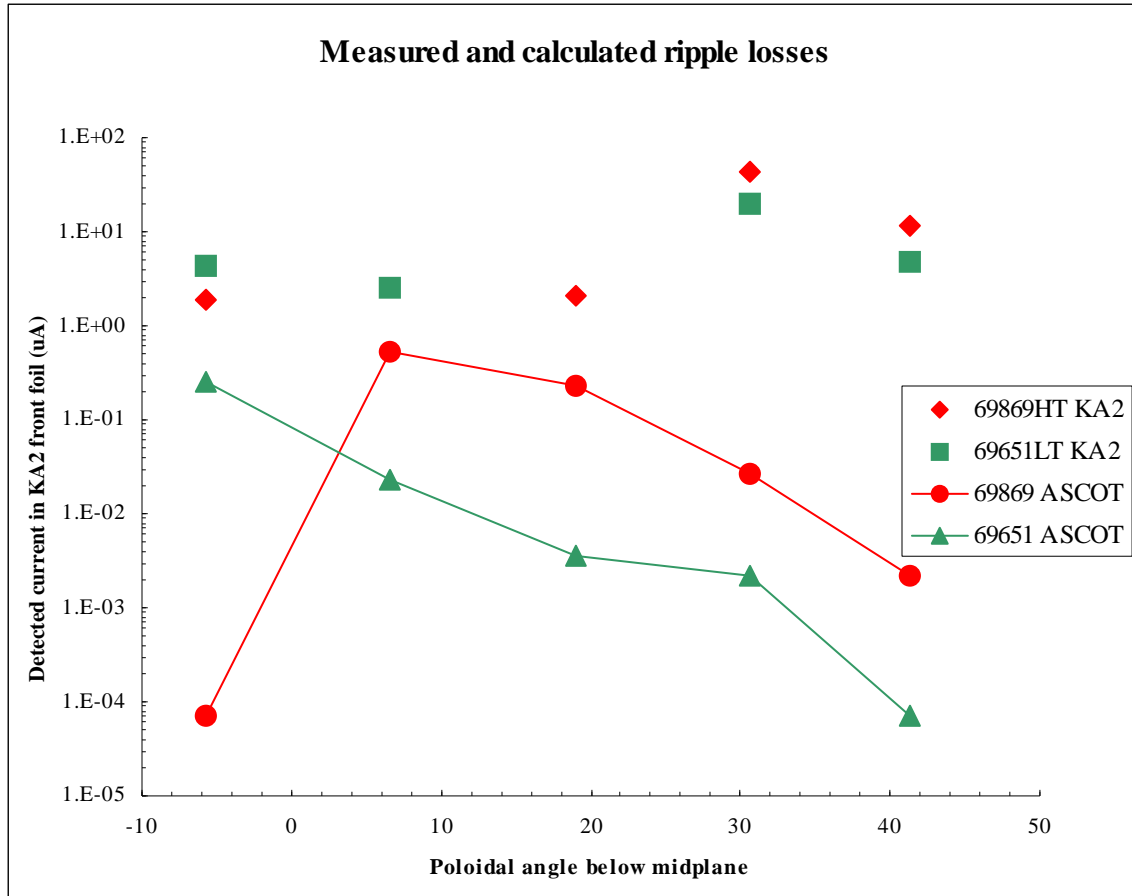


Figure 15 Comparison of calculated and measured quiescent currents in the 5 front foils of KA2 during the H-mode phase of the JET plasmas 69869 and 69651. These plasmas were, respectively high and low triangularity plasmas with a TF ripple of 1 %.

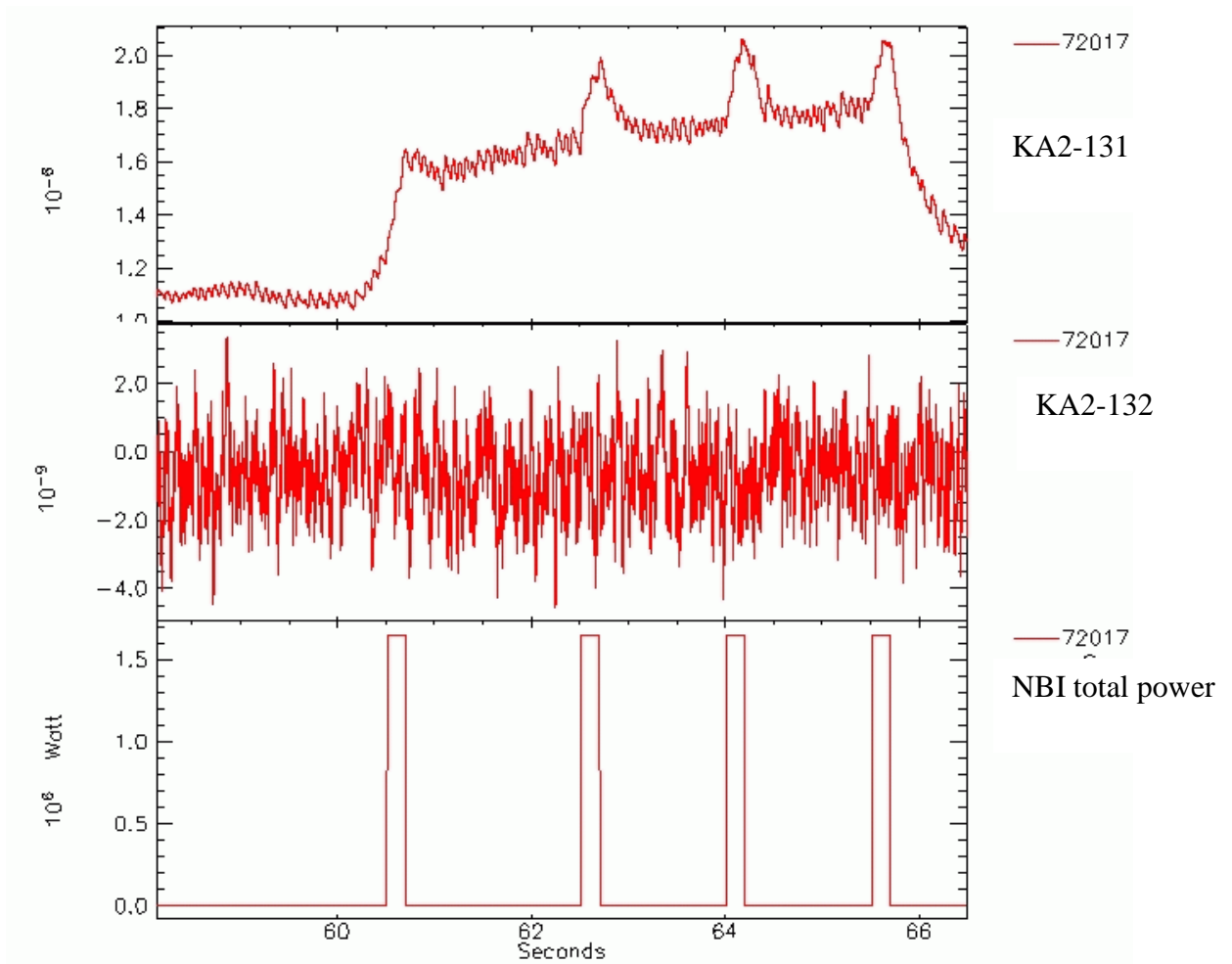


Figure 16. Comparison of front and interior foils of KA2 during Ohmic plasma with NBI blips illustrating that the quiescent background signal in the interior foil ($I_{\text{rms}} < 1 \text{ nA}$) is unaffected by the currents in the front foil.